World Journal of Engineering and Technology, 2026, 14(4), 1111-1139
https://www.scirp.org/journal/wjet
ISSN Online: 2331-4249
ISSN Print: 2331-4222

Thermodynamic Performance Analysis of a Low-Cost Sand-Silo Thermal Battery with Indirect Solar Heating

Javed Ahmed Khan Tipu[1*], Adnan Aslam Noon[2], Muhammad Arif[1], Omar A. Beg[3*], Abbas Raza[4], Altaf Khan[4], Azhar Ul Islam Zafar[5], Muhammad Shaharyar[1], Aisha Ahmed Khan[1], Zimad Ahmed Khan[6]

[1]Faculty of Engineering and Technology, International Islamic University, Islamabad, Pakistan
[2]Department of Mechanical Engineering, Khawaja Farid University of Engineering and Information Technology, Rahim Yar Khan, Pakistan
[3]College of Engineering and Sciences, The University of Texas Permian Basin, Odessa, TX, USA
[4]Global Competency Certification Agency. Pvt. Ltd., Islamabad, Pakistan
[5]AIMS Group of Companies, Islamabad, Pakistan
[6]Wah Engineering College, University of Wah, Wah, Pakistan
Email: *javed.ahmed@iiu.edu.pk, *beg_o@utpb.edu

How to cite this paper: Tipu, J.A.K., Noon, A.A., Arif, M., Beg, O.A., Raza, A., Khan, A., Zafar, A.U.I., Shaharyar, M., Khan, A.A. and Khan, Z.A. (2026) Thermodynamic Performance Analysis of a Low-Cost Sand-Silo Thermal Battery with Indirect Solar Heating. *World Journal of Engineering and Technology*, **14**, 1111-1139.
https://doi.org/10.4236/wjet.2026.144066

Received: September 4, 2026
Accepted: November 24, 2026
Published: November 27, 2026

Copyright © 2026 by author(s) and Scientific Research Publishing Inc.
This work is licensed under the Creative Commons Attribution International License (CC BY 4.0).
http://creativecommons.org/licenses/by/4.0/
Open Access

Abstract

This study describes a prototype sand-silo thermal store heated indirectly by an evacuated-tube solar collector and copper coil. The reported prototype contains approximately 307.5 kg of silica sand. In one nine-hour charging sequence, the recorded sand-probe temperature increased from 34.1˚C to 42.7˚C and water temperature from 34.9˚C to 65.1˚C. Using the reported sand mass, an assumed sand specific heat of 830 $J{\cdot}kg^{-1}{\cdot}K^{-1}$, and the recorded sand-probe temperature change gives a provisional sensible-energy estimate of 2.195 MJ (0.61 kWh), conditional on that probe representing the bulk bed. The nominal-flow-based HTF energy estimate is 9.791 MJ; their ratio is 22.4%, but this is not a closed-system or solar-collector efficiency. Irradiance, collector aperture area, calibrated flow measurement, spatial sand-temperature mapping, and component energy accumulation were not documented. The recalculated 63.2% water-rise target is 54.0˚C and is first exceeded at approximately 90 minutes. Only one charging cycle is available. Simulation maxima (about 87˚C in the text and 95˚C in the figure legend) do not quantitatively agree with the recorded sand-probe maximum of 42.7˚C. Findings are preliminary prototype observations; repeatability and quantitative simulation validation are not established.

Keywords

Renewable Energy, Sand Silo, Heat Transfer Fluid, Thermal Energy Storage, Solar Thermal System

1. Introduction

Thermal energy storage (TES) is an essential technology for boosting the use of renewable energy because it stores excess heat and releases it when needed. Over the past 20 years, several TES technologies have been investigated, including phase change materials (PCMs), molten salts, and packed-bed storage systems. Zalba *et al.* [1] highlighted the potential of low-cost storage materials in their review of different thermal energy storage technologies. Farid *et al.* discussed latent heat storage and practical applications of phase change materials [2]. Diago *et al.* [3] studied sand-based packed-bed storage and highlighted its thermal stability at high temperatures, even though insufficient heat transfer remained a major barrier. The benefits of sand, such as its accessibility, affordability, and thermal stability, were also covered by Kenisarin and Mahkamov [4]. Emphasized the availability and thermal stability of sand while highlighting the need to integrate sand with solar collectors, building on the previously mentioned study. In a more recent study, [5] investigated seasonal heat storage in cold climate sand beds. Budihardjo and Morrison [6] evaluated evacuated-tube solar water heaters, while Xu *et al.* [7] studied sand saturated with thermally conductive fluid. Barbi *et al.* [8] investigated sand-PCM mixtures in greater detail to boost heat storage capacity.

Research on the effectiveness of sand-based thermal energy storage systems has been ongoing. Yousef *et al.* [9] evaluated a sand-based storage unit through experimental analysis, while Niksiar *et al.* [10] investigated the effect of copper fins on the heat-transfer efficiency of silica sand. Pinto and Beausoleil-Morrison [11] developed and experimentally validated a numerical model for seasonal sand-based heat storage, while Ma *et al.* [12] investigated long-duration particle thermal energy storage using silica sand. More experimental research is needed to evaluate small-scale systems and improve heat transfer, even though these studies demonstrate that sand has the potential to be a reliable and affordable storage material.

To address the lack of small-scale field observations, this study describes a prototype sand-silo thermal store heated indirectly by an evacuated-tube solar collector and copper coil under the reported climate conditions of Islamabad. One nine-hour charging sequence is available. The reported sand-probe temperature rose from 34.1˚C to 42.7˚C and the water temperature from 34.9˚C to 65.1˚C. A provisional sand sensible-energy estimate can be calculated, but the data do not establish a closed-system efficiency, validated time constants, quantitative simulation agreement, or repeatability. This manuscript therefore treats the results as preliminary observations and identifies the measurement and design information required for further validation.

2. Literature Review

Sand has been thoroughly studied as a readily available and reasonably priced material for thermal energy storage (TES), particularly for solar thermal applications. Diago *et al.* [3], who emphasized the beds' potential for high-temperature heat storage. Evacuated-tube solar water heaters were assessed by Budihardjo and

Morrison [6], who also showed how well they collected solar heat. In their review of various thermal energy storage materials, Kenisarin and Mahkamov [4] emphasized the benefits of sand, such as its accessibility, thermal stability, and affordability. Xu *et al.* [7] investigated the heat storage capacity of sand mixed with a thermally conductive fluid and compared it to concrete. Hailu *et al.* [5] investigated seasonal heat storage in sand beds in cold climates. Similarly, Barbi *et al.* [8] investigated seasonal heat storage in sand beds in cold climates. Recent research has looked more closely at the potential of sand-based thermal energy storage systems. Yousef *et al.* [9] evaluated a sand-based storage unit through experimental analysis and response surface methodology. Pinto and Beausoleil-Morrison developed and experimentally validated a numerical model for seasonal sand-based heat storage [11]. Ma *et al.* [12] investigated components for long-duration thermal energy storage using silica sand. Additionally, Niksiar *et al.* [11] looked into the thermal performance of silica sand and the effect of copper fins on improving heat transfer. Overall, previous research has shown that sand is a promising material for thermal energy storage due to its affordability, accessibility, and thermal stability. However, improving heat transfer and evaluating the effectiveness of small-scale storage systems remain important research areas. Specifically, there hasn't been much experimental research done on systems that combine evacuated-tube solar collectors with sand-silo thermal energy storage. Therefore, developing and testing an integrated evacuated-tube solar collector and sand-silo storage system is the aim of this study. Its potential for efficient solar heat storage will be assessed, along with its thermal performance. A summary of the relevant research studies is given in Table 1.

Table 1. Summary of last 10 relevant research papers (2009-2024).

Sr. No	Year	Author(s)	Findings
1	2018	Diago, M., Iniesta, A. C. [3]	Highlighted the potential of desert sand for solar thermal applications and described it for high-temperature thermal energy storage.
2	2009	Budihardjo, I., [6]	Assessed the thermal performance of evacuated-tube solar water heaters.
3	2007	Kenisarin, M., & Mahkamov, K. [4]	Examined the use of phase-change materials in solar thermal energy storage.
4	2017	Xu, B., Han, J., Kumar, A. [7]	Examined the performance of sand saturated with a heat-conductive fluid and contrasted it with concrete.
5	2017	Hailu, G., Hayes, P. [5]	Seasonal solar heat storage in sand beds in cold climates was investigated experimentally.
6	2021	Barbi, S., Barbieri, F. [8]	Investigated and assessed the thermal performance of sand-PCM mixtures for thermal energy storage.
7	2024	Yousef, B. A. A., Radwan, A. [9]	Used response surface methodology and experimental analysis to assess a sand-based thermal energy storage device.
8	2023	Pinto, R. I. [11]	Created a numerical model for seasonal sand-based thermal energy storage and verified it experimentally.
9	2022	Ma, Z., Wang, X. [12]	Using silica sand, components for long-duration particle thermal energy storage were developed and tested.
10	2024	Niksiar, P., Rogillio, C. [10]	Investigated silica sand thermal storage experimentally and looked at how copper fins affected heat-transfer efficiency.

The low cost and thermal stability of sand have been emphasized in previous investigations which have demonstrated the feasibility of thermal energy storage using sand and sand battery solar thermal energy storage. Nevertheless, all these studies have mentioned various constraints due to poor heat transfer and stratification especially for small sizes. There is an obvious gap of experimentally validated small-size sand silos with complete thermal and thermodynamic analysis due to the focus on hybrid systems and large-scale sand batteries in the latest literature.

3. Methodology

The process for investigating heat transfer and temperature distribution started with the design of a sand silo thermal battery in SolidWorks software and analysis of this design in ANSYS work bench software. The prototype used the evacuated tube solar collector as the source of heat input with a copper coil heat exchanger embedded in sand. The theoretical modeling of energy storage, exergy analysis, and heat transfer were included in support of simulations and experimental work. The experiments were performed in Islamabad to evaluate efficiency, U value, and energy storage in natural solar conditions.

3.1. Feasibility and Conceptual Design

The initial step towards the methodology was conducting feasibility studies of the thermal properties of sand, such as its density, specific heat, and conductivity. As a result of this, a design concept was developed that would optimize the size of the silo, the type of materials used for the walls, and the thickness of the insulation. The final design drawings were then done using SolidWorks.

3.2. Market Survey

In order to examine the viability of sand-silo thermal batteries in comparison to current batteries, a market survey was carried out. This survey was performed with respect to the availability of the materials required for high-temperature operation, as well as insulation and instrumentation. The pros of using such batteries included their cost-effectiveness and efficiency.

3.3. Fabrication Process

The fabrication involved multiple stages:

1. **Design completion:** through SolidWorks drawings and ANSYS testing.
2. **Material collection:** tank, insulation layers, copper tubing, and sensors.
3. **Foundation building:** building a foundation to support the silo.
4. **Tank construction:** construction and reinforcement of the tank.
5. **Installation of insulation:** installing insulation in the inner and outer layer.
6. **Heat exchanger installation:** installing copper tubing and pipes.
7. **System assembly:** incorporation of pumps, collectors, and blowers.
8. **Performance monitoring:** installation of sensors for performance analysis.

3.4. Component Selection

The tank shell is said to be made up of fiber reinforced material, with foam and glass-wool for insulation. Sand was used as the heat storage material, and the indirect heating system was made up of a pump, evacuated tube collector, and copper coil. There are sensors that measured temperature, but calibration and placement of sensors are unknown.

3.5. Solar Evacuated Tube Collector

In the evacuated tube collector, borosilicate glass tubes and Al-N/Al absorber coating were employed as indicated in the design details. The claim made by the manuscript earlier regarding the solar energy collector efficiency above 92% has not been supported through the measurement of the irradiance and useful gain values and thus has not been taken as the measurement of the thermal efficiency. No pyranometer/solarimeter data, calibration certificate, and actual value of the collector aperture area have been provided for the experimental results. The collector was mounted at a tilt angle of 18.7˚ in Islamabad during the summer season. The evacuated tube solar collector used in the prototype is presented in Figure 1.



Figure 1. Evacuated tube collector.

3.6. Working Fluid

Water was used as the heat-transfer fluid (HTF) for the indirect-heating experiment. All calculations that use fluid properties therefore assume liquid water, with approximate density 1000 $kg \cdot m^{-3}$ and specific heat 4184 $J \cdot kg^{-1} \cdot K^{-1}$ over the temperature range considered. A nominal circulation rate of 10 L/min (approximately 0.1667 kg/s when treated as water) appears in the original records, but the flow-measurement method and calibration are undocumented; consequently, all flow-dependent heat-rate and integrated-energy values are estimates, not traceable measurements.

3.7. Sensors and Instrumentation

The temperatures of sand, circulating water, pipe inlet and outlet, room air, and

outer/collector related point were taken every 15 minutes. The recorded information does not provide any information on location coordinates of sensors, depth of insertion, number of sand probes used, type of sensors used, and method of calibration. These cannot be reconstructed; thus, they are mentioned as limitations. The temperatures of the pipe inlet and outlet were found to be the same up to 35.7˚C up to 11:30. Then there was a sharp change to 50.1˚C and 49.8˚C after 11:45. It implies that there was no heat rate generated in the beginning because of the zero-temperature difference. It could not be said that the heat is being transferred from HTF to the sand. The sudden change may be because of any transcription error, delay in the circulation, or sensor behavior. The only thing that can be inferred is heat rate calculation conditionally based on any valid temperature difference.

3.8. Copper Coiling and Piping

The design of the source describes a 500-inch (12.7 m) copper coil, 13 turns, the diameter of the ring being 12 in., spacing of 6.25 in., and a ring radius of 6.125 in. These dimensions are mutually inconsistent with the reported 33-in tank height: 13 turn centers at 6.25-in pitch span 75 in between the first and last centers, before end clearances. A 6.125-in radius corresponds to a 12.25-in diameter, not 12 in. The as-built coil geometry is therefore unverified. Coil surface area, heat-transfer coefficient, and simulation results that depend on this geometry are provisional and should not be interpreted as validated until the drawing and fabricated coil are reconciled. The copper-coil configuration is illustrated in Figure 2.



Figure 2. Copper coils.

3.9. Insulated Sand-Silo Tank

The sand-silo is 33 inches tall and 22 inches in diameter, with a nominal volume of 0.205 m^3. Layers of foam and glass-wool served as insulation. The available ex-

periment did not quantify their contribution to lowering heat loss.

3.10. Water Pump

In order to guarantee continuous circulation of hot water coming from the evacuated tube collector into the copper coil, the use of a circulation pump was considered. This guarantees that there will be no stagnation and thus heat transfer will constantly occur. The pump is designed to withstand pressures ranging from 1.4 to 4.8 bar with a maximum pressure of 6 bar. Circulation pump used to maintain HTF flow is presented in Figure 3.



Figure 3. Water pump.

3.11. Blower for Heat Extraction

The heat would be drawn out of the system through the use of a blower that forced air through the hot sand bed. Given the flexibility of heat extraction methods, this system demonstrated the possibility of utilizing the silo for low-grade industrial or space heating. The blower employed for heat extraction is presented in Figure 4.



Figure 4. Blower (For heat extraction).

3.12. Insulation Layers

In order to reduce heat loss through convection and conduction, the tank was insulated using foam boards and glass wool wraps. This was important for ensuring that there were no fluctuations in the temperature of the sand, thus ensuring efficiency of the system. Insulation arrangement applied to the tank is illustrated in Figure 5.

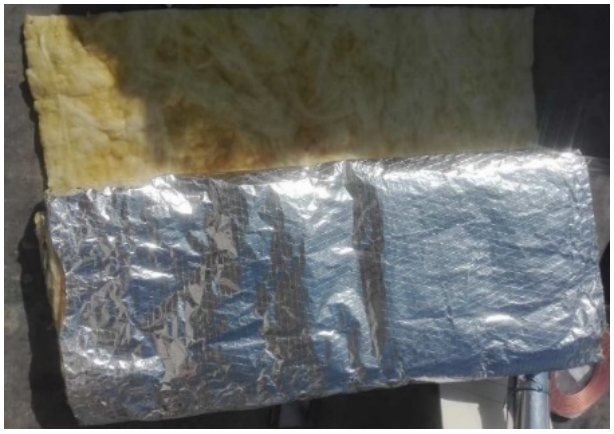

Figure 5. Glass wool insulation.

3.13. Modeling and Simulation Work

A 3D SolidWorks model for the sand-silo and copper coil system was developed for preliminary analysis. After importing this model to ANSYS Workbench, meshing and transient thermal simulation was performed. The simulations provided data on heat transfer coefficient, stratification, and temperature distribution which helped in optimizing the design. For obtaining correct results, the problems associated with meshing and solution setup had to be corrected. The principal model dimensions are reported in Table 2. Corresponding SolidWorks models of the silo and coil are presented in Figure 6 and Figure 7, respectively.



Figure 6. 3D model of copper coils in solid-works.



Figure 7. 3D model of sand-silo thermal battery in solid-works.

Table 2. Dimensions for 3D model.

No.	Element	Specifications
1.	length of Tank	33 inches
2.	Diameter of Tank	22 inches
3.	Volume of Tank	12544 in3
4.	Size of Copper Piping	¼ (0.25)
5.	Length of Copper Piping	500 inches
6.	Number of Rings	13 turns
7.	Ring Diameter	12 inch & 6.125 in radius
8.	Ring Center-To-Center Distance	6.25 inch; implies ~75 in span for 13 turn centers
9.	Ring Radius	6.125 inch; implies 12.25 in diameter
10.	Pitch Diameter	1.615 inches

3.13.1. Work Simulation

Numerical Modeling was performed using ANSYS Workbench (R18.2) to determine the distribution of heat in the sand silo and verify the results of the experiment. Figure 8 shows the geometry of the cylindrical silo that has been meshed. Thermal mapping throughout the domain was guaranteed through structured meshing. Computational mesh generated for the silo model is illustrated in Figure 9.

3.13.2. Steady State Thermal Stress

The ANSYS output is a modeled temperature distribution, and not a measured one. There is a reported local maximum value of about 87˚C in the manuscript text, while there seems to be a local maximum of about 95˚C indicated in the Fig-

ure 10 legend. Both these values exceed the highest value measured by the sand probe of 42.7˚C, and also do not correlate with each other. Since there is no documentation for geometry, boundary conditions, material properties, and so on, the modeling is exploratory in nature.

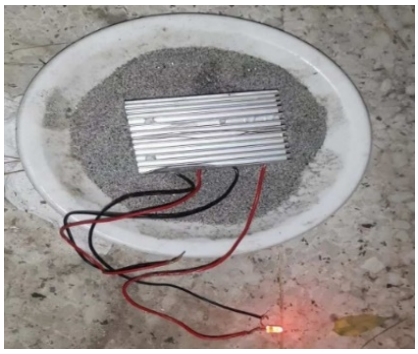

Figure 8. Working of thermo-electric generator setup.

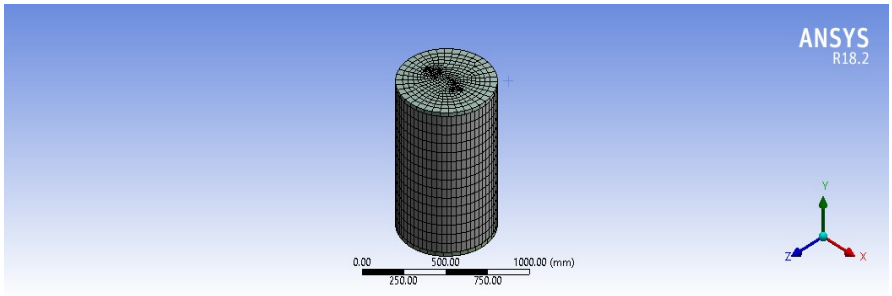

Figure 9. Meshing of sand-silo thermal battery in ANSYS.

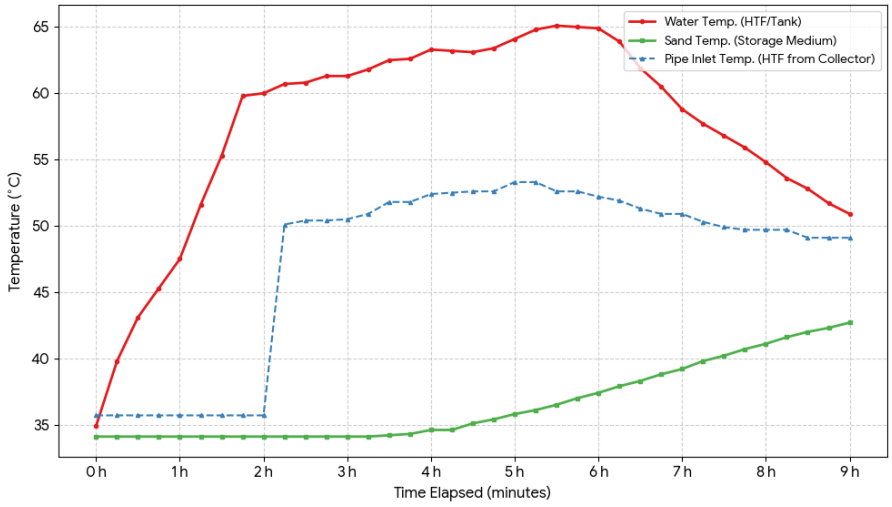

Figure 10. Experimental data of indirect heating method.

3.14. Theoretical Formulations

The intended calculations include sensible energy storage, HTF heat-transfer rate, and thermal response indicators. Solar irradiance, collector aperture area, a documented irradiance measurement method, and collector inlet/outlet en-

ergy balance are not available in the source records. Accordingly, solar input and collector thermal efficiency are not calculated as measured quantities. Sand sensible energy is estimated from Q = mc_pΔT, subject to the limitation that the reported sand temperature change may not represent a spatially averaged bulk temperature.

4. Design and Performance Calculations

The calculation and evaluation of the performance of the sand-silo thermal battery system are outlined in this section. The principles of thermodynamics, theoretical equations, and experimental data form the basis of calculations. The performance parameters such as stored energy, rate of heat transfer, efficiency, exergy, and discharge capacity are evaluated to assess the performance of the system.

4.1. Mass of Sand and Stored Sensible Energy

The reported sand mass is 307.5 kg and the reported sand-probe temperature changes from 34.1˚C to 42.7˚C. Applying the assumed sand specific heat of 830 $J \cdot kg^{-1} \cdot K^{-1}$ gives a provisional sensible-energy increase of 2.195 MJ (0.61 kWh), but this estimate assumes the single reported sand temperature represents the bulk bed. The number and locations of sand probes are not documented, so the spatial representativeness of this estimate is unknown. It is not a measured total-system storage value. Sand mass and associated provisional sensible-energy estimate are reported in Table 3.

Table 3. Mass & stored energy.

Quantity	Formula/Step	Numeric Work	Value
Tank volume	$V = 12.544\ in^3 \times (0.0254)^3$		0.205 m^3
Sand density	Given	-	1500 kg/m^3
Sand mass	$m = \rho V$	0.205×1500	307.5 kg
ΔT (sand)	Tf-Ti	42.7 - 34.1	8.6 K
Stored energy	Q = mcpΔT	$307.5 \times 830 \times 8.6$	2.195 MJ

4.2. Heat Transfer Fluid (HTF) Energy Input

The integrated HTF energy estimate is 9.79 MJ when the nominal flow rate and recorded pipe temperature differences are used. This number depends upon the unverified value of 10 L/min, as well as the accuracy of the inlet and outlet measurements, including the jump at 11:45. This is not an actual input to the solar collector. The reported 976 W peak follows from the sample at 13:00 (51.8 - 50.4 = 1.4 K) and the assumed flow rate; it should be interpreted as an estimate rather than a validated heat rate. The estimated energy transferred by the heat-transfer fluid (HTF) is reported in Table 4.

Heat transfer fluid (HTF) in the solar collector helps in transferring heat. Energy flow:

Table 4. HTF energy.

Quantity	Formula / Step	Numeric Work	Value
Mass flow	Given	$\dot{m}$ = 10 L/min = 0.1667 kg/s	0.1667 kg/s (assumed; flow method undocumented)
Specific heat	Given	-	4184 J/kg·K
Example ΔT	Tin-Tout	51.8 - 50.4	1.4 K
$\dot{Q}$ (sample)	$\dot{m}$cpΔT	0.1667 × 4184 × 1.4	976 W (conditional estimate)
Energy (15 min)	$\dot{Q}$ × 900	976 × 900	0.879 MJ per 15 min at 976 W; conditional estimate
Total HTF energy	ΣEi	-	9.791 MJ (integrated estimate; not measured solar input)

4.3. Instantaneous Heat Transfer Rates

The estimates of the heat transfer rate for HTF at any particular instant are made using the pipe temperature differences recorded and the nominal water flow rate assumed. Since flow calibration is not documented and early inlet/outlet readings are identical, the derived peak (976 W) and mean (294 W across all samples; 389 W across positive-ΔT samples) values are not traceable measurements. They shouldn't be taken as proof of consistent heat transfer. Calculated HTF heat-transfer rates are presented in Table 5.

Table 5. Heat transfer rates.

Quantity	Formula	Value
Peak $\dot{Q}$	max $\dot{Q}$i	976 W (conditional estimate)
Mean $\dot{Q}$ (all data)	Σ$\dot{Q}$i/N	294 W (derived from recorded ΔT and assumed flow)
Mean $\dot{Q}$ (ΔT > 0)	average of positive samples	389 W (derived estimate; positive-ΔT samples only)
Total energy	Σ$\dot{Q}$I × 900	9.791 MJ (estimate; not measured input)

4.4. Effective Heat Transfer Coefficient (U-Value)

There is not enough data to come up with an acceptable value of the overall heat transfer coefficient between the coil and sand. An accepted value of the coil area, accurate inlet and outlet temperatures, an accurate value of the flow rate, and an acceptable sand temperature are needed to compute this, but these values are not all available. Thus, the previous values of 228 W/m²·K and 116 W/m²·K are only saved as interim computations and are not used to support any performance claims. The assumptions and results of the provisional overall heat-transfer-coefficient calculation are presented in Table 6.

Table 6. U-value.

Quantity	Formula/Step	Numeric Work	Value
Coil area	A = πdL	0.00635 × π × 12.7	0.253 m² (based on unverified coil geometry)
ΔT1, ΔT2	Tin-Ts, Tout-Ts	17.6 K, 16.2 K	-
LMTD	ΔT1 - ΔT2 / ln(ΔT1/ΔT2)	-	16.89 K
U (sample #15)	$\dot{Q}$/(AΔTlm)	976/(0.253 × 16.89)	228 W/m²·K (provisional; geometry/flow uncertain)
Mean U	Average of valid samples	-	116 W/m²·K (provisional; not validated)

4.5. Thermal Response Time Constants

The 63.2% temperature-rise level is calculated as $T_{63.2} = T_i + 0.632(Tf - T_i)$. The calculation for water gives 34.9 + 0.632 (65.1 - 34.9) = 54.0 °C, and the first sample that is above this temperature is 55.3˚C, which is at 11:00, 90 minutes after the experiment began. The calculation for sand gives 34.1 + 0.632 (42.7 - 34.1) = 39.5˚C, and the first sample that exceeds this temperature is 40.2˚C at 17:00. These are sampled response indicators only. They are not validated first-order time constants because the solar input was not measured and cannot be assumed constant, and the sand temperature may not be spatially representative. Calculated 63.2% temperature-rise thresholds and corresponding sampled response times are reported in Table 7.

Table 7. Time constants.

Material	Initial-Final (˚C)	Target 63.2% (˚C)	Time reached	T
Water	34.9 - 65.1	54.0	~90 min (first sample > target)	Response indicator; not τ
Sand	34.1 - 42.7	39.5	~450 min (first sample > target)	Response indicator; not τ

4.6. Charge Efficiency and Energy Balance

The reported sand sensible-energy increase is Q_sand = mc_pΔT = 307.5 × 830 × (42.7 - 34.1) ≈ 2.195 MJ, conditional on the measured temperature change representing the bulk sand. The 9.791 MJ HTF figure is an estimate based on nominal flow and recorded inlet/outlet temperature differences. The closed energy balance cannot be determined since the irradiation value and collector aperture surface are not known, and the energy stored in the circulating fluid, copper coil, tank body, and insulation material were not determined. Hence, 2.195/9.791 = 22.4% is only an approximation of the ratio of the estimated sensible energy gain in the sand to the estimated heat transfer fluid energy, and not the collector efficiency or charging efficiency of the closed system. The energy difference of 7.596 MJ is left unaccounted for. The provisional energy estimates and their ratio are reported in Table 8. The system-level energy-flow representation is provided in Figure 11.

4.7. Exergy and Entropy Analysis

A constant control volume, a known reference environment, an accurate measure of mass flow rate and temperature, and a sealed or measured energy balance are required for exergy and entropy analysis. The records that are currently available do not meet those requirements. Therefore, it is not appropriate to interpret the previously determined exergy and entropy values as measured exergy efficiency or experimentally quantified irreversibility because they are merely exploratory. Exploratory exergy and entropy estimates are reported in Table 9.

Table 8. Energy balance.

Quantity	Formula	Value
Energy in (HTF)	∑Q˙Δt	9.791 MJ (estimated from assumed flow and recorded ΔT)
Energy stored (sand)	mcΔT	2.195 MJ (provisional; assumes probe ΔT represents bulk sand)
Charge efficiency	Qsand/QHTF	22.4% provisional ratio only; not a closed-system or collector efficiency

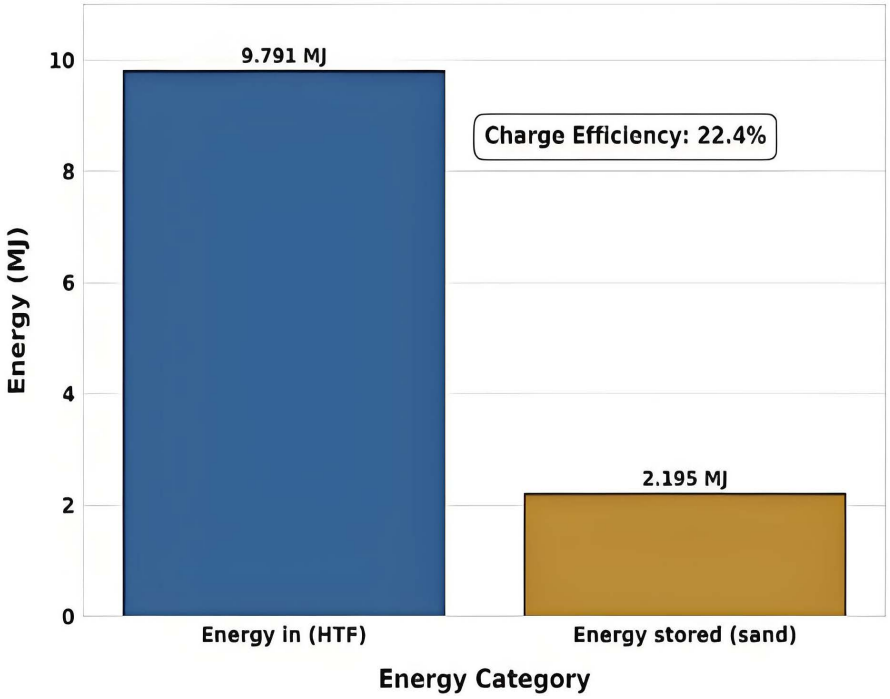

Figure 11. System energy balance.

Table 9. Exergy analysis.

Quantity	Formula	Value
Ambient temp.	-	309.15 K
Exergy in (HTF)	∑Ei(1 - T0/Tavg)	0.454 MJ
Exergy stored	mcΔT - T0mc ln(Tf/Ti)	0.0168 MJ
Exergy destroyed	Exin-Exstored	0.437 MJ
Entropy generation	mc ln(Tf/Ti)	7046 J/K

4.8. Energy Densities

The primary limitation of the provisional energy-density values, which are arithmetic transformations of the sand sensible-energy estimate, is that the spatially averaged bed may not be represented by the single reported sand-probe temperature change. They should not be used to argue that they are better than other thermal storage media because they are not verified system-level storage metrics. Derived gravimetric and volumetric energy-density estimates are reported in Table 10.

Table 10. Energy densities.

Metric	Formula	Value
Volumetric density	Q/V	10.7 MJ/m^3
Specific energy	Q/m	7.1 kJ/kg (1.98 Wh/kg)
Reference (salts)	-	80 - 100 MJ/m^3

4.9. Average Discharge Power

There is no measured discharge curve or direct forced-air discharge test available. The preliminary energy value obtained for sand was then divided by the discharge times to give values of 84 W and 102 W, which are approximate computations and not measurements of discharge power. The approximate discharge-power estimates, calculated from the provisional stored energy, are reported in Table 11.

Table 11. Discharge power.

Discharge Window	Formula	Value
6-hour discharge window	Q/t	102 W
7.25-hour window	Q/t	84 W

4.10. Measurement Uncertainty

There is only one recorded instance of nine hours of charging process. There are no independent repetitions of charging process, therefore, inter-cycle variability, repeatability, and statistical robustness cannot be determined. Information on solar irradiation uncertainty, sensor calibration information, location of sensors, number of sand probes and their locations, and the validated flow metering technique is lacking. The aforementioned uncertainties of HTF energy and sand energy of ±27.6% and ±8.2% respectively are estimated rather than actual uncertainty budget. Provisional uncertainty estimates and their underlying assumptions are reported in Table 12.

Table 12. Uncertainty.

Quantity	Formula/Step	Value
ΔT uncertainty	Sqrt ($0.5^2 + 0.5^2$)	0.71 K (sensor accuracy)
Sand energy error	mcσT	±0.18 MJ (provisional estimate)
HTF sample error	$\dot{m}c\sigma T\Delta t$	±0.44 MJ per sample
Total HTF error	sqrt(N) dEs, N = 37	±2.70 MJ (27.6%; provisional)

5. Testing and Experimental Validation

The test of the prototype took place in Islamabad during a single solar charging run that lasted for nine hours, with temperature data collected at an interval of every 15 minutes. There is no information available regarding the solar irradiance measuring device, location and orientation of the measurement, calibration, error, and aperture area of the collector from the source records. The temperature time

series available can describe the measured behavior only.

5.1. Direct Heating Method

For another proof-of-concept test using the direct heating approach, a ceramic pot was equipped with thermoelectric generators, LEDs, and an electric heater rated at 1000 W. Inasmuch as no calibrated energy balance data exists for this setup in the existing record, its efficiency cannot be calculated and only described qualitatively. Principal components of the direct-heating demonstrator are listed in Table 13.

Table 13. Components used in direct heating method.

Name of Equipment	Quantity
Ceramic Container	01
Ceramic Plate	01
Wires	02
LEDs	02
Heat Sink	02
Electric Heater (1000 W)	01
Thermoelectric Generators	02
Thermal Conductive Paste	01

It was also observed from the experiment that the sand was a logical thermal energy storage material since it could directly absorb heat from the heat source. Furthermore, there existed a temperature difference between the heat sink and the heated sand, and this allowed the TEGs to generate power, and in the process, light up the LED lights.

5.2. Limitations of Direct Heating

Despite the proof-of-concept, several challenges were observed:

- Uneven heat distribution across the sand resulted in thermal inefficiency.
- Stratification of the heat produced hot and cold spots.
- Degradation of materials happened owing to frequent heating.
- Adherence of sand to heating surfaces hampered conductivity.
- Heat losses were due to poor insulation.

This drawback necessitated the use of indirect heating through solar thermal collectors, providing a more controlled and scalable means of charging the sand bed.

5.3. Indirect Heating Method

Water was circulated between the evacuated-tube collector and the copper coil embedded in the sand during the indirect-heating experiment. Water is the only HTF assumed throughout this manuscript. Temperature data were recorded at 15-minute intervals, but sensor locations, sand-probe count and placement, calibration, and flow-measurement method were not documented. The nominal 10 L/min flow rate is therefore an assumption, and heat-rate/energy values derived

from it are provisional.

5.3.1. Materials Needed

1. Collector (evacuated tube type)
2. Heat transfer fluid (water)
3. Insulated storage tank
4. Pump for circulating heat transfer fluid
5. Heat exchanger (copper coil)
6. Sample of sand (quantity to be determined)
7. Thermocouples (sand, water, pipe inlet/outlet)
8. Insulation (glass wool, foam)
9. Pipes and pipe fittings
10. Sun's irradiance measurement and tilting arrangement

5.3.2. Procedure

1. The solar collector was installed at an optimal angle (18.7˚ in Islamabad).
2. Water was circulated between the collector and the coil.
3. The sand container was indirectly heated through the copper coil.
4. Temperature was recorded at intervals of 15 minutes.
5. Temperatures were taken every 15 minutes while water was moved between the copper coil and the evacuated-tube collector. Because the two configurations were not compared using a common, measured energy boundary, the available record does not prove that this process was more efficient than direct heating.

Although the intended heat-transfer pathway is demonstrated by the indirect-heating arrangement, the available measurements did not quantitatively demonstrate uniform heating, increased efficiency, or decreased risk.

5.3.3. Working

Heat transfer occurs between the circulating fluid, which is the HTF, and the evacuated tube collector that collects solar radiation. Heat conduction will be used to transfer energy from the wall of the pipes into the sand particles as hot water is pumped into copper pipes embedded in the sand bed. The temperature of the sand bed increases with time due to its role as a thermal reservoir. To make sure that efficient charging takes place, the system will be insulated to prevent heat loss. The ability of the battery to sustain thermal energy release during discharge is shown by passing fluids or air through the sand bed. Experimental arrangement incorporating thermoelectric generators is illustrated in **Figure 8**.

5.4. Experimental Results

Temperature records for the indirect-heating test cover 09:30 - 18:30 at 15-minute intervals. The measured temperature of the water rose from 34.9˚C to 65.1˚C, whereas the measured temperature of the sand rose from 34.1˚C to 42.7˚C. The highest measured outer temperature was 43.8˚C at 13:00. Because irradiance data are not available, the temperature changes cannot be associated numerically with a solar radiation flux. The sand temperature is calculated based on an unknown probe config-

uration. Recorded water and sand-probe temperatures are tabulated in Table 14 and measured temperature histories during the charging test are plotted in Figure 10.

Table 14. Experimental data of indirect heating method.

SR #	Time	Room (T)	Outer (T)	Water (T)	Sand (T)	Pipe Inlet (T)	Pipe Outlet (T)
1	9:30	34	38.9	34.9	34.1	35.7	35.7
2	9:45	34.3	39	39.8	34.1	35.7	35.7
3	10:00	34.4	39.1	43.1	34.1	35.7	35.7
4	10:15	34.4	40	45.3	34.1	35.7	35.7
5	10:30	34.4	40.9	47.5	34.1	35.7	35.7
6	10:45	34.5	39.1	51.6	34.1	35.7	35.7
7	11:00	34.6	40.5	55.3	34.1	35.7	35.7
8	11:15	34.7	40.5	59.8	34.1	35.7	35.7
9	11:30	35.2	40.9	60	34.1	35.7	35.7
10	11:45	35.4	40.2	60.7	34.1	50.1	49.8
11	12:00	35.3	41.1	60.8	34.1	50.4	49.8
12	12:15	35.6	41.5	61.3	34.1	50.4	49.9
13	12:30	35.8	41.6	61.3	34.1	50.5	49.9
14	12:45	35.7	41.7	61.8	34.1	50.9	49.9
15	13:00	35.6	43.8	62.5	34.2	51.8	50.4
16	13:15	36.1	42.8	62.6	34.3	51.8	50.9
17	13:30	35.9	42.6	63.3	34.6	52.4	51.8
18	13:45	35.9	41.9	63.2	34.6	52.5	51.8
19	14:00	36	41.7	63.1	35.1	52.6	52
20	14:15	35.8	42.5	63.4	35.4	52.6	52
21	14:30	35.9	42.8	64.1	35.8	53.3	52.7
22	14:45	35.8	43.1	64.8	36.1	53.3	52.7
23	15:00	36	42.3	65.1	36.5	52.6	52
24	15:15	36	42.4	65	37	52.6	52
25	15:30	36.1	41.6	64.9	37.4	52.2	52
26	15:45	36.1	40.9	63.9	37.9	51.9	51.3
27	16:00	36.2	39.8	61.9	38.3	51.3	50.9
28	16:15	36.2	39.8	60.5	38.8	50.9	50.2
29	16:30	36.2	39.7	58.8	39.2	50.9	50.2
30	16:45	36.2	38.9	57.7	39.8	50.3	50
31	17:00	36.2	39.3	56.8	40.2	49.9	49.5
32	17:15	36.2	39.1	55.9	40.7	49.7	49.3
33	17:30	36.2	38	54.8	41.1	49.7	49.3

Continued

34	17:45	36.2	37.8	53.6	41.6	49.7	49.4
35	18:00	36.2	36.5	52.8	42	49.1	48.7
36	18:15	36.2	35.7	51.7	42.3	49.1	48.8
37	18:30	36	33.9	50.9	42.7	49.1	48.8

6. Results and Discussion

From one charging event recorded in this experiment, an increase in the sand temperature of 8.6˚C was observed. From this information and using the specified sand mass and heat capacity value, an estimated energy increase of 2.195 MJ (0.61 kWh) is obtained. The 9.79 MJ HTF value and the subsequent 22.4% ratio are only estimates and cannot be considered to represent the charging efficiency of the system. Thermal efficiency of the collector, energy balance calculation, exergetic considerations, and coil to sand heat transfer coefficient have not been validated due to lack of data on irradiance, aperture size, and flow measurement. The reported 84 - 102 W discharge values are calculated estimates, not measured discharge performance.

6.1. Experimental Validation at Small Scale

This work provides preliminary prototype-scale observations from one recorded charging sequence in a nominal 0.205 m^3 silo. The sand-temperature change implies a provisional sensible-energy increase of 2.195 MJ (0.61 kWh) only if the reported temperature change represents the bulk sand. One sequence does not establish repeatability, statistical reliability, or general suitability for residential/off-grid applications. Additional calibrated measurements, repeated cycles, and direct discharge tests are required before such performance claims can be made. The principal measured temperatures and derived preliminary storage estimate are summarized in Table 15. Figure 12 presents the derived stored-energy relationship, while Figure 13 shows the estimated HTF energy trend.

6.2. Improved Heat Transfer with Optimized Coil Geometry

The design description includes a 500-inch copper coil, with 13 turns, but the pitch and ring size are inconsistent with the 33-inch tank size and each other. The as-built configuration of the coil should be confirmed before the area and heat-transfer coefficient of the coil to sand are considered credible. The estimated range from 37 to 228 $W/m^2 \cdot K$ and the 116 $W/m^2 \cdot K$ average are based on the assumed coil area and nominal flow rate, along with dubious initial pipe measurements. The provisional heat-transfer-coefficient estimates are compared in Table 16. Calculated distribution of provisional heat-transfer-coefficient values is presented in Figure 14.

Table 15. Energy storage performance.

Parameter	This Work	Previous Research Trend	Improvement
Stored energy (per cycle)	2.195 MJ one cycle)	Not comparable from the information available	Preliminary single-cycle observation
Prototype volume	0.205 m^3	Not established	Nominal prototype scale; performance not validated
Proof of feasibility	Preliminary temperature rise observed	Varies by study	Repeatability not established

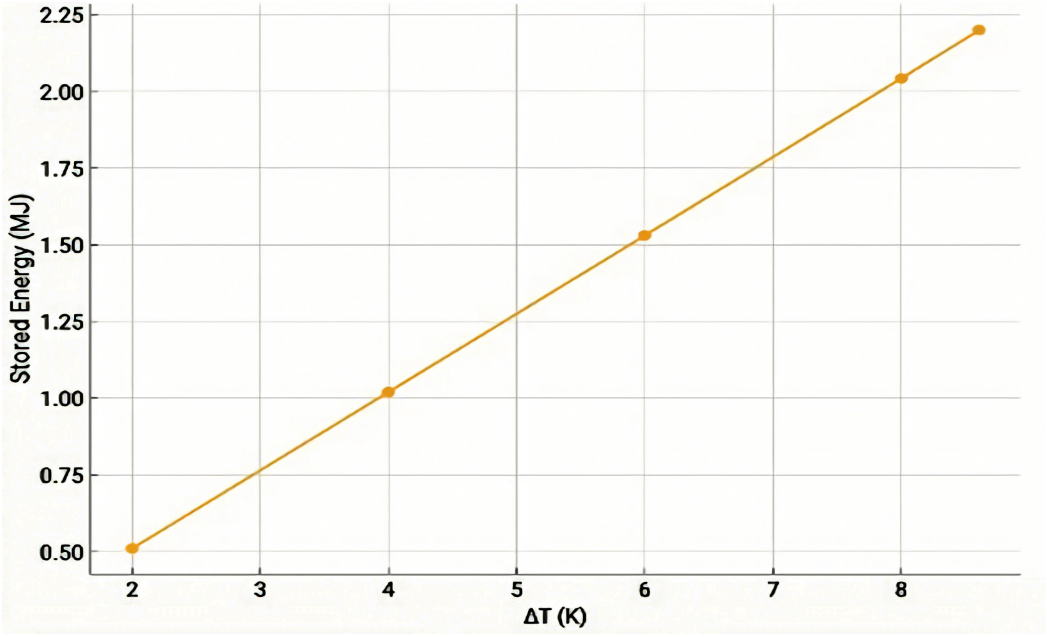

Figure 12. Stored energy and temperature relation.

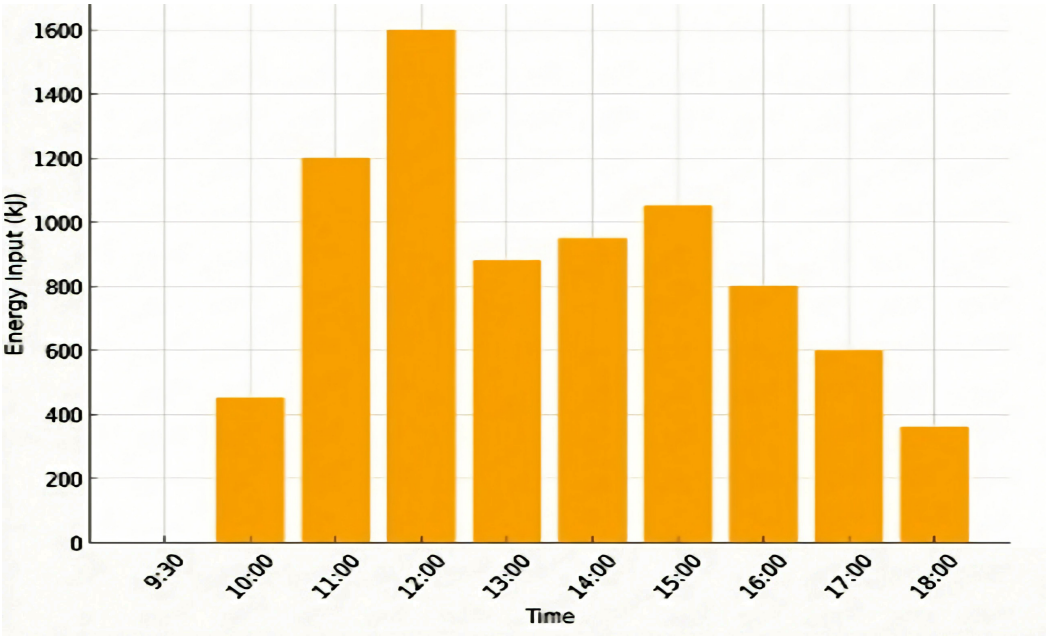

Figure 13. HIF energy with time.

Table 16. Heat transfer coefficient comparison.

Parameter	This Work	Previous Research Trend	Improvement
U-value range	37 - 228 W/m²·K (provisional calculation)	Not compared on a consistent basis	No improvement claim supported
Average U-value	116 W/m²·K (provisional)	Not available on a consistent basis	Requires verified geometry and measurements
Design strategy	Coil geometry reported but inconsistent	Not evaluated	As-built geometry must be verified

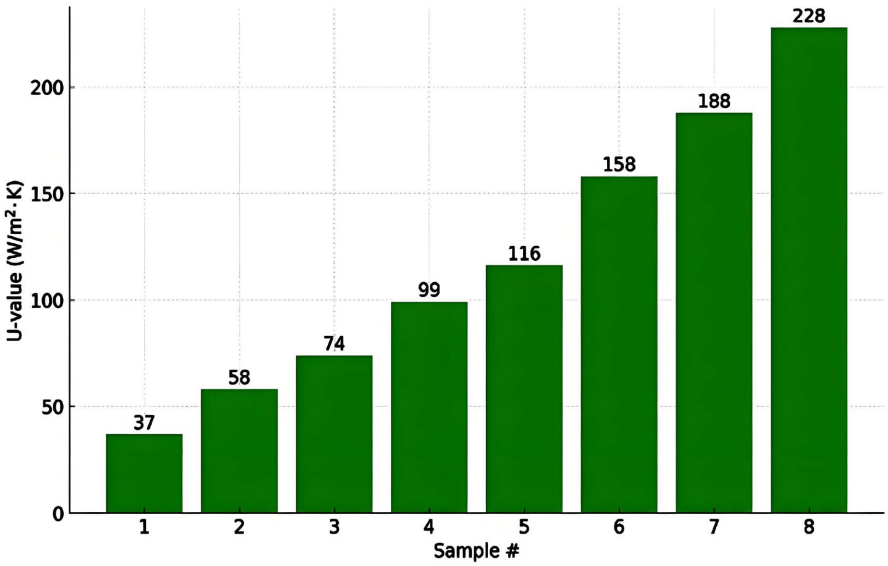

Figure 14. Heat transfer coefficient distribution.

6.3. Charging Efficiency and Energy Loss Mechanisms

The estimated HTF energy and the assumed bulk sand energy increase are used to calculate the provisional ratio of 22.4%, which should not be interpreted as a full system charging efficiency. There was insufficient data on solar irradiance, collector aperture area, collector inlet/outlet energy balance, and the energy stored in the water, coil, tank, and insulation to close the overall balance. As a result, the apparent discrepancy between the estimated HTF input and the sand sensible-energy gain is unallocated; the measurements available do not allow for its separation into tank/pipe storage and external losses. No mechanism is given an unsupported percentage of loss.

6.4. Exergy Analysis and Irreversibility

The exergy values previously reported (including 0.454 MJ input, 0.0168 MJ stored, and 3.7% efficiency) depend on the assumed HTF flow, temperature data, reference state, and simplified boundary. Because the underlying HTF energy input and component energy balance are not validated, these values should be treated as exploratory calculations rather than experimentally established exergy efficiency or quantified exergy destruction. The available data do not isolate the

individual causes of irreversibility.

6.5. Real-Time Dynamic Behavior Captured

The temperature records show different observed trends for water and the sand probe during one nine-hour test. The water response indicator reaches its calculated 63.2% rise target at the first sample above 54.0˚C (approximately 90 minutes after the start); the sand probe first exceeds its 39.5˚C target at approximately 450 minutes. These values are response indicators, not validated time constants. The data do not show that the water loop stabilized in 45 minutes or that the sand reached a validated time constant of 7.25 hours. The sampled response indicators for the water and sand-probe temperature histories are reported in Table 17. Figure 15 presents the sampled thermal-response analysis, and Figure 16 shows the corresponding temperature profiles.

6.6. Discharge Performance

Discharge power estimates (84 - 102 W) in this paper do not employ direct forced-air discharge tests but rather calculate based on the storage energy divided over a realistic discharge period. The complete discharge tests have been out of the scope of this research project although a heat extraction system based on the use of a blower was installed. Nevertheless, such an estimate of the discharge power can be considered a practical approach to estimate the heating capacity of the system. Future research will provide experimental discharge curves including air temperature decay and power drop.

Table 17. Thermal response.

Material	Initial Temp	Final Temp	Time Constant (τ)	Key Advantage
Water	34.9˚C	65.1˚C	~90 min to first sampled crossing; response indicator only	Observed water temperature rise
Sand	34.1˚C	42.7˚C	~450 min to first sampled crossing; response indicator only	Observed sand-probe rise; spatial mean unknown

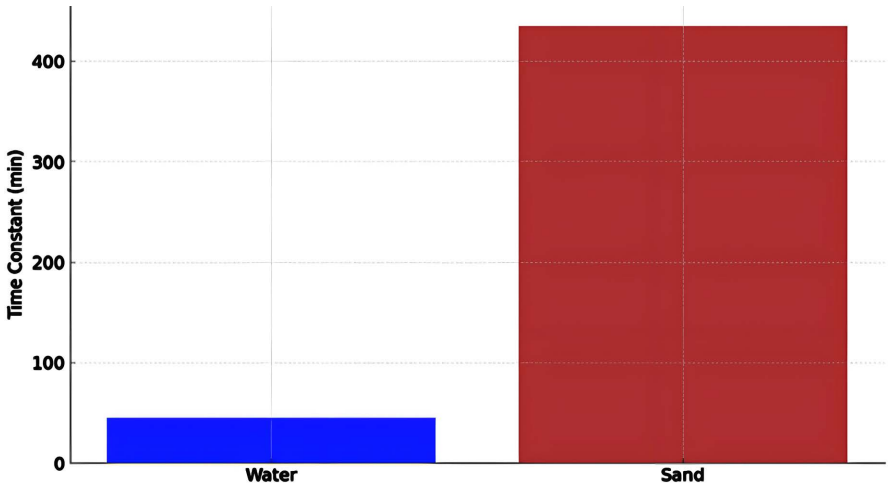

Figure 15. Time response.

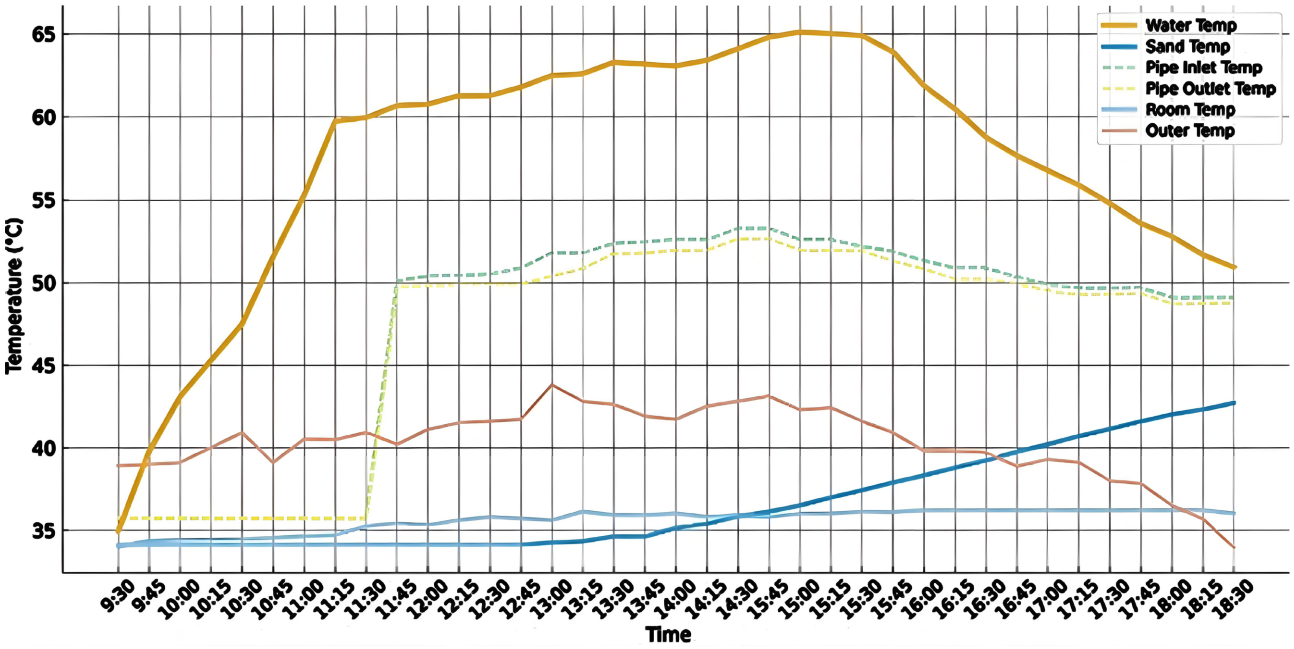

Figure 16. Temperature profile.

6.7. Quantification of Exergy Destruction

The exergy calculations are retained only as exploratory estimates because the input energy, spatial sand temperature, and component energy accumulation are not adequately measured. The numerical values of exergy input, stored exergy, destroyed exergy, and efficiency should not be interpreted as validated experimental results. A defensible second-law analysis requires a consistent control volume, documented reference environment, reliable mass flow and temperature measurements, and a closed or explicitly quantified energy balance. Exploratory exergy estimates are reported in Table 18. Provisional charge-efficiency and exploratory exergy results are visualized in Figure 17 and Figure 18, respectively.

Table 18. Summary of exploratory exergy estimates and their validation status.

Parameter	Value in This Work	Typical in Previous Work	Improvement
Exergy input (HTF)	0.454 MJ (exploratory estimate; not validated)	Exploratory estimate only; not validated	No improvement claim supported
Exergy stored in sand	0.0168 MJ (exploratory estimate; not validated)	Exploratory estimate only; not validated	Requires a defensible control volume and measurements
Exergy destroyed	0.437 MJ (exploratory estimate; not validated)	Exploratory estimate only; not validated	Not established experimentally
Exergy efficiency	3.7% (exploratory estimate; not validated)	Exploratory estimate only; not validated	Not established experimentally

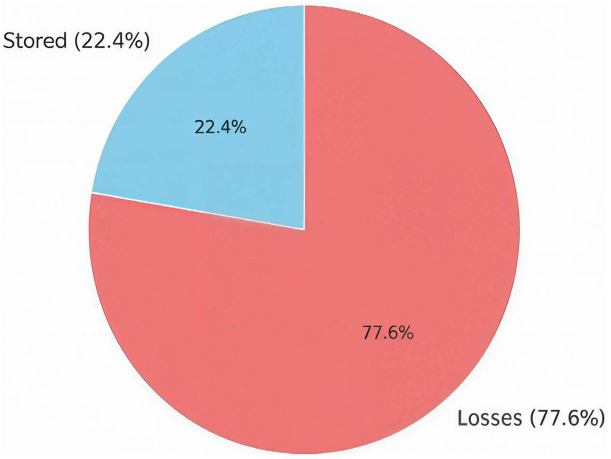

Figure 17. Charge efficiency.

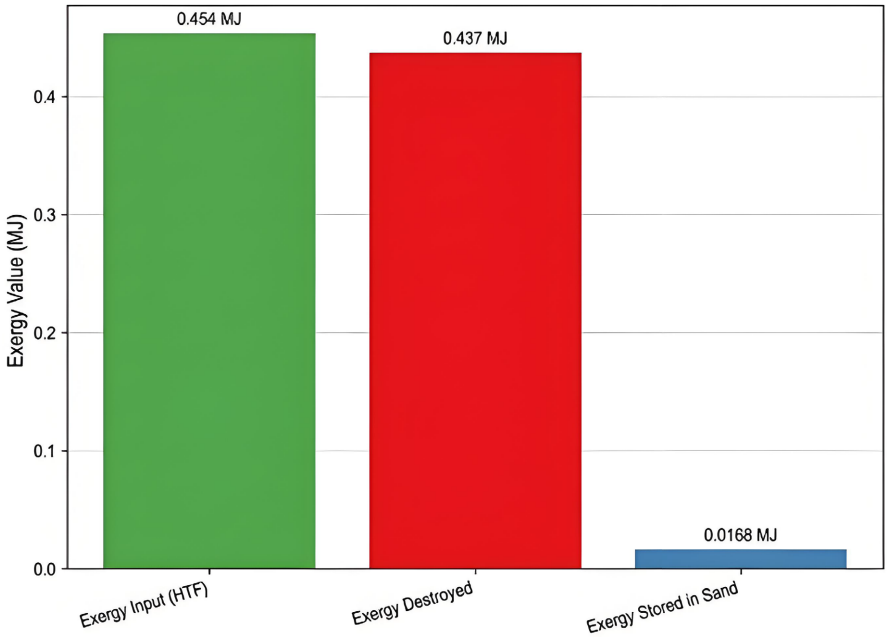

Figure 18. Exergy distribution of the system.

6.8. Simulation vs. Experimental Comparison

This study describes the design, first simulation, and one recorded charging sequence of a sand-silo thermal store with a copper-coil heat exchanger. Applying the stated sand mass and assumed specific heat to the reported 8.6˚C increase in sand-probe temperature yields a provisional sensible-energy estimate of 2.195 MJ (0.61 kWh), conditional on the probe representing the bulk bed. The nominal-flow-based heat-transfer-fluid (HTF) energy estimate is approximately 9.79 MJ, and the 22.4% ratio is not a closed-system charging efficiency. Quantitative validation is not established because the measured sand-probe maximum of 42.7˚C does not match the simulation maxima reported in the text (about 87˚C) and figure legend (about 95˚C). Repeated testing, recorded irradiance and collector aperture area, calibrated sensors and flow measurement, spatial sand-temperature

mapping, component energy accounting, and verified coil geometry are all necessary before performance or reliability claims can be made.

6.9. Practical Energy Density and Discharge Potential

The specific energy density and volumetric energy density stated above are derived mathematically from the preliminary estimation of 2.195 MJ and the mass or volume of the system. The assumption made above is that the temperature change of the individual sand grains represents the entire bed. The values 84 to 102 W are also mathematically estimated using discharge time and not tested during discharge power test. Derived energy-density and estimated discharge-power values are reported in Table 19 and Figure 19 and Figure 20.

6.10. Cost-Effective and Sustainable Design

The prototype employs readily available materials like sand and copper pipes that could perhaps provide a cheap way to go about the design process. But there is no cost analysis or any performance validation of the storage technology, as well as a lack of data that would prove performance through single cycle measurements to be outstanding or better than any other storage mechanism. Qualitative assessment of cost and practical implementation considerations is presented in Table 20 and Figure 21.

Table 19. Energy density and discharge.

Metric	This Work	Previous Research Trend	Improvement
Volumetric density	10.8 MJ/m^3 (based on provisional sand energy)	Not compared on a consistent basis	Preliminary estimate
Specific energy	1.98 Wh/kg (based on provisional sand energy)	Not compared on a consistent basis	Preliminary estimate
Average discharge power	84 - 102 W (calculated, not measured)	Not established	Direct discharge test required

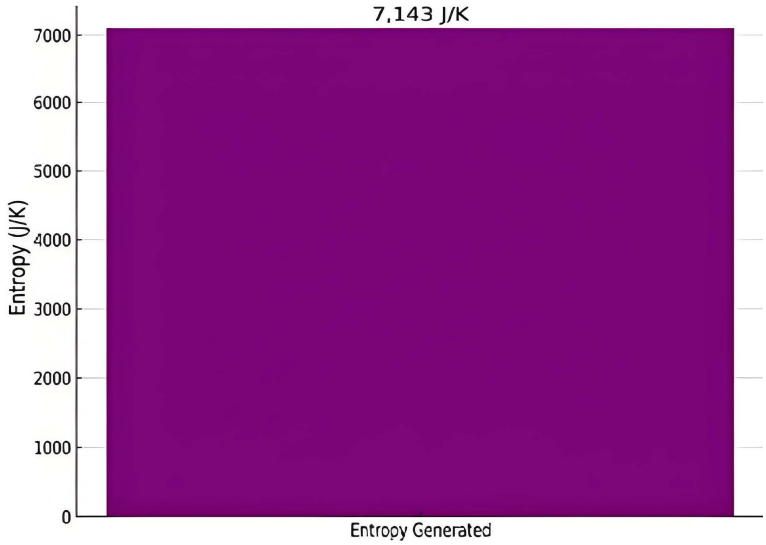

Figure 19. Energy generation.

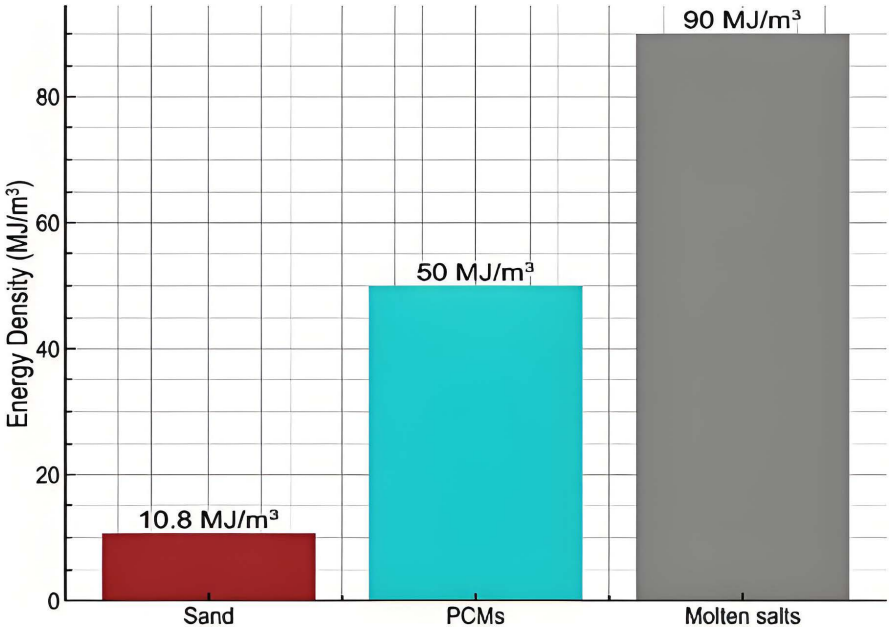

Figure 20. Energy density comparison.

Table 20. Cost and practicality.

Factor	This Work	Previous Research Trend	Improvement
Material choice	Sand + copper	Sand + PCM composites	Potential low-cost option; cost not quantified
Complexity	Simple design	High-tech composites	Simple component selection; comparative analysis not performed
Suitability	Domestic/rural	Industrial only	Potential application only; not demonstrated

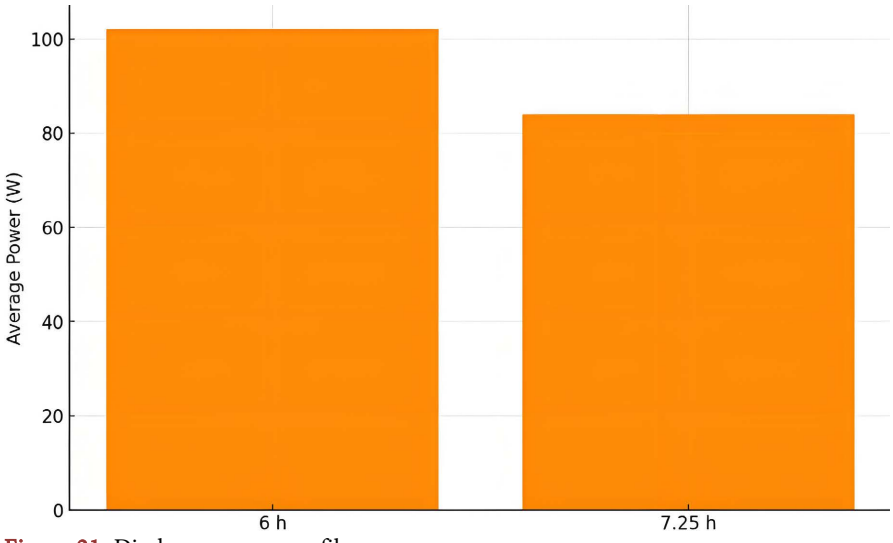

Figure 21. Discharge power profile.

6.11. Simulation vs. Experiment Comparison

This study describes the design, preliminary simulation, and one recorded charging sequence of a sand-silo thermal store with a copper-coil heat exchanger. The reported sand-probe temperature rose by 8.6˚C; applying the stated sand mass

and assumed specific heat yields a provisional sensible-energy increase of 2.195 MJ (0.61 kWh), conditional on that probe representing the bulk bed. The nominal-flow-based HTF energy estimate is 9.79 MJ, giving a provisional ratio of 22.4%, not a closed-system charging efficiency. The reported simulation maxima (approximately 87˚C in the text and 95˚C in the figure legend) do not agree with the measured sand-probe maximum of 42.7˚C, so quantitative validation is not established. Repeated charging tests, irradiance and aperture-area measurements, calibrated sensors and flow measurement, spatial sand-temperature mapping, component energy accounting, and verified coil geometry are needed before performance or reliability claims can be made. The current research outlines the design, initial simulation, and one documented charging cycle of the thermal energy storage using sand silo with a copper coil heat exchange system. In the present research, the increase in the temperature of the sand probe was 8.6˚C and, based on the given sand mass and specific heat, the approximate sensible energy increase is 2.195 MJ (0.61 kWh), provided that the sand probe gives the temperature of the entire bed. The nominal flow basis gives the energy input of HTF as 9.79 MJ, and hence the provisional percentage of energy increase is 22.4% which is not the charging efficiency in a closed system. There is no agreement between the maximum temperatures from the simulation (approximately 87˚C from the text and 95˚C from the figure caption) and the maximum temperature in the sand probe (42.7˚C). Hence, there is no validated energy increase at this stage.

6.12. Measurement Limitations and Scope of Interpretation

There is only one recording of nine hours of charge data. There is no mention of the method used for measuring solar irradiance or its values, area of collector aperture, irradiance uncertainty, calibration of sensors, exact location of sensors, sand probe counts and location, and the validation of flow metering method. These factors do not allow any estimation of solar collector efficiency, energy balance, or repeatability of data. The unaccounted difference between energy in HTF and provisional energy in sand cannot be attributed solely to the losses as there was no estimation of energy storage in water, coil, tank, and insulation. Coil parameters are inconsistent within themselves. Simulation results have only exploratory value.

7. Conclusion and Future Work

The design of the prototype device and one observed charging cycle show a recorded rise in the reported sand probe temperature from 34.1˚C to 42.7˚C. The associated energy content of 2.195 MJ (0.61 kWh) is based on the assumption that this temperature rise accounts for all 307.5 kg of sand. The HTF energy content of 9.79 MJ and efficiency of 22.4% are provisional values based on the undetermined nominal flow rate and pipe temperature data; 22.4% is not a validated efficiency. The heat transfer coefficient, exergy, and discharge power values are provisional or calculated, not independently verified.

In future investigations, it will be necessary to resolve the discrepancies between the real coil dimensions and those on the tank design drawing, followed by repeating the charging test, using calibrated temperature sensors and a flow meter. The amount of incoming solar energy should be measured using a calibrated pyranometer or solarimeter at the plane of the collector, and the size of the collector aperture should be documented, allowing the analysis of the collector thermal efficiency. Several sand probes should be set up at known locations in order to find the spatially averaged temperature. The energy balance should include the changes in the energy of water, coil, tank shell, insulation, and sand, while the rest of the residual energy will remain unallocated, unless loss terms are estimated separately.

Author Contributions

Javed Ahmed Khan Tipu and Adnan Aslam Noon contributed to conceptualization and methodology; Muhammad Arif, Abbas Raza, Altaf Khan, and Azhar Ul Islam Zafar contributed to technical development and research activities; Omar A. Beg contributed to supervision and critical review; Muhammad Shaharyar contributed to experimental work, data analysis, and manuscript preparation; Aisha Ahmed Khan and Zimad Ahmed Khan contributed to research support and manuscript revision. All authors reviewed and approved the final manuscript.

Conflicts of Interest

The authors declare no conflicts of interest regarding the publication of this paper.

References

[1] Zalba, B., Marín, J.M., Cabeza, L.F. and Mehling, H. (2003) Review on Thermal Energy Storage with Phase Change: Materials, Heat Transfer Analysis and Applications. *Applied Thermal Engineering*, **23**, 251-283. https://doi.org/10.1016/s1359-4311(02)00192-8

[2] Farid, M.M., Khudhair, A.M., Razack, S.A.K. and Al-Hallaj, S. (2004) A Review on Phase Change Energy Storage: Materials and Applications. *Energy Conversion and Management*, **45**, 1597-1615. https://doi.org/10.1016/j.enconman.2003.09.015

[3] Diago, M., Iniesta, A.C., Soum-Glaude, A. and Calvet, N. (2018) Characterization of Desert Sand to Be Used as a High-Temperature Thermal Energy Storage Medium in Particle Solar Receiver Technology. *Applied Energy*, **216**, 402-413. https://doi.org/10.1016/j.apenergy.2018.02.106

[4] Kenisarin, M. and Mahkamov, K. (2007) Solar Energy Storage Using Phase Change Materials. *Renewable and Sustainable Energy Reviews*, **11**, 1913-1965. https://doi.org/10.1016/j.rser.2006.05.005

[5] Hailu, G., Hayes, P. and Masteller, M. (2017) Seasonal Solar Thermal Energy Sand-Bed Storage in a Region with Extended Freezing Periods: Part I Experimental Investigation. *Energies*, **10**, Article 1873. https://doi.org/10.3390/en10111873

[6] Budihardjo, I. and Morrison, G.L. (2009) Performance of Water-in-Glass Evacuated Tube Solar Water Heaters. *Solar Energy*, **83**, 49-56. https://doi.org/10.1016/j.solener.2008.06.010

[7] Xu, B., Han, J., Kumar, A., Li, P. and Yang, Y. (2017) Thermal Storage Using Sand

Saturated by Thermal-Conductive Fluid and Comparison with the Use of Concrete. *Journal of Energy Storage*, **13**, 85-95. https://doi.org/10.1016/j.est.2017.06.010

[8] Barbi, S., Barbieri, F., Marinelli, S., Rimini, B., Merchiori, S., Larwa, B., *et al.* (2021) Phase Change Material-Sand Mixtures for Distributed Latent Heat Thermal Energy Storage: Interaction and Performance Analysis. *Renewable Energy*, **169**, 1066-1076. https://doi.org/10.1016/j.renene.2021.01.088

[9] Yousef, B.A.A., Radwan, A., Haridy, S. and Alajmi, N. (2024) Performance Evaluation of a Sand Energy Storage Unit Using Response Surface Methodology. *Energy*, **289**, Article 129885. https://doi.org/10.1016/j.energy.2023.129885

[10] Niksiar, P., Rogillio, C., Torab, H. and Tiari, S. (2024) Experimental Study of a Silica Sand Sensible Heat Storage System Enhanced by Fins. *Energies*, **17**, Article 5402. https://doi.org/10.3390/en17215402

[11] Pinto, R.I. and Beausoleil-Morrison, I. (2023) Experimental Validation of a Numerical Model for a Sand-Based Seasonal Thermal Energy Storage. *Journal of Building Performance Simulation*, **16**, 644-659. https://doi.org/10.1080/19401493.2023.2191338

[12] Ma, Z., Wang, X., Davenport, P., Gifford, J., Cook, K., Martinek, J., *et al.* (2022) System and Component Development for Long-Duration Energy Storage Using Particle Thermal Energy Storage. *Applied Thermal Engineering*, **216**, Article 119078. https://doi.org/10.1016/j.applthermaleng.2022.119078